


ORIGINAL RESEARCH

NADPH oxidase 4 deficiency attenuates experimental osteoarthritis in mice

Félix Renaudin ^{1,2}, Karim Oudina,^{1,2} Maude Gerbaix,³ Manon McGilligan Subilia,^{1,2} Joris Paccaud,^{1,2} Vincent Jaquet,⁴ Karl-Heinz Krause,⁴ Serge Ferrari,³ Thomas Laumonier,^{1,2} Didier Hannouche^{1,2}

To cite: Renaudin F, Oudina K, Gerbaix M, *et al.* NADPH oxidase 4 deficiency attenuates experimental osteoarthritis in mice. *RMD Open* 2023;**9**:e002856. doi:10.1136/rmdopen-2022-002856

Received 10 November 2022
Accepted 18 January 2023



© Author(s) (or their employer(s)) 2023. Re-use permitted under CC BY-NC. No commercial re-use. See rights and permissions. Published by BMJ.

¹Department of Cell Physiology and Metabolism, Université de Genève Faculté de médecine, Geneva, Switzerland

²Department of Orthopaedic Surgery, Geneva University Hospitals, Geneva, Switzerland

³Service of Bone Diseases, Department of Medicine, Geneva University Hospitals, Geneva, Switzerland

⁴Department of Pathology and Immunology, Université de Genève Faculté de médecine, Geneva, Switzerland

Correspondence to

Professor Didier Hannouche;
Didier.Hannouche@hcuge.ch

ABSTRACT

Objective Low-grade inflammation plays a pivotal role in osteoarthritis (OA) through exposure to reactive oxygen species (ROS). In chondrocytes, NADPH oxidase 4 (NOX4) is one of the major ROS producers. In this study, we evaluated the role of NOX4 on joint homeostasis after destabilisation of the medial meniscus (DMM) in mice. **Methods** Experimental OA was simulated on cartilage explants using interleukin-1 β (IL-1 β) and induced by DMM in wild-type (WT) and NOX4 knockout (NOX4^{-/-}) mice. We evaluated NOX4 expression, inflammation, cartilage metabolism and oxidative stress by immunohistochemistry. Bone phenotype was also determined by micro-CT and histomorphometry.

Results Whole body NOX4 deletion attenuated experimental OA in mice, with a significant reduction of the OARSI score at 8 weeks. DMM increased total subchondral bone plate (SB.Th), epiphyseal trabecular thicknesses (Tb.Th) and bone volume fraction (BV/TV) in both NOX4^{-/-} and wild-type (WT) mice. Interestingly, DMM decreased total connectivity density (Conn.Dens) and increased medial BV/TV and Tb.Th only in WT mice. Ex vivo, NOX4 deficiency increased aggrecan (AGG) expression and decreased matrix metalloproteinase 13 (MMP13) and collagen type I (COL1) expression. IL-1 β increased NOX4 and 8-hydroxy-2'-deoxyguanosine (8-OHdG) expression in WT cartilage explants but not in NOX4^{-/-}. In vivo, absence of NOX4 increased anabolism and decreased catabolism after DMM. Finally, NOX4 deletion decreased synovitis score, 8-OHdG and F4/80 staining following DMM.

Conclusion NOX4 deficiency restores cartilage homeostasis, inhibits oxidative stress, inflammation and delays OA progression after DMM in mice. These findings suggest that NOX4 represent a potential target to counteract for OA treatment.

INTRODUCTION

Articular cartilage is a non-vascularised and non-innervated tissue that exhibits a limited capacity of self-regeneration.¹ In healthy cartilage, extracellular matrix (ECM) turnover is slow, while in osteoarthritis (OA),^{2,3} cartilage degradation predominates over cartilage repair, leading to cartilage fibrillation, thinning and calcification in patients. In response to abnormal mechanical loading

WHAT IS ALREADY KNOWN ON THIS TOPIC

⇒ Inflammation and oxidative stress are two major components of osteoarthritis pathophysiology.

WHAT THIS STUDY ADDS

⇒ This study demonstrated that for the first time that NADPH oxidase 4 (NOX4) is necessary for the progression osteoarthritis after destabilisation of the medial meniscus surgery. NOX4 is major component of joint inflammation and oxidative stress in osteoarthritis.

HOW THIS STUDY MIGHT AFFECT RESEARCH, PRACTICE OR POLICY

⇒ These findings identify NOX4 as a potential target for osteoarthritis treatment.

or joint injury, chondrocytes contribute to the synthesis of proinflammatory cytokines and the release of catabolic enzymes such as A disintegrin And metalloproteinase with thrombospondin motifs (ADAMTS), cathepsin K, aggrecanases (Agg) and matrix metalloproteinases (MMP) which alter ECM.^{4,5} The decreased synthesis of collagen type II (COL2) and proteoglycans during OA is accompanied by an upregulation of MMP, ADAMTS as well as expression of type X collagen (COL10), a marker of hypertrophic chondrocytes.⁵ Although the exact mechanism driving these processes is not fully understood, it is likely that chronic inflammation plays a crucial role in hypertrophic differentiation of chondrocytes through the release of inflammatory cytokines such as interleukin (IL)-1 β , TNF- α or IL-6.⁶

Accumulating evidence points to the role of reactive oxygen species (ROS) in the regulation and progression of OA.^{7,8} ROS act as signalling intermediates in the activation of different pathways in osteoarthritic chondrocytes, disrupting their normal structure and function, and leading to cytotoxicity. Among the different ROS, H₂O₂ appears to be a key

regulatory molecule as it exerts similar effects on chondrocytes *in vitro* as IL-1 β .⁹ ROS inhibit anabolic activities of chondrocytes, upregulate the production of MMP^{10,11} and promote articular cartilage degeneration in OA.^{11,12} Moreover, mechanical stress leads to oxidation of cartilage glutathione diminishing its capacity to protect cartilage from oxidative stress.¹³ It has been demonstrated that oral administration of the antioxidant N-acetyl cysteine in rats inhibits cartilage degradation, and reduces MMP13 and TNF- α expression.¹⁴ Altogether, ROS inhibition seems to be a promising therapeutic target in OA.¹⁵

Sources of ROS consist of different cellular organelles such as peroxisomes, endoplasmic reticulum and mitochondria. Another important source of ROS are plasma membrane-associated oxidases, the NADPH oxidases (NOX), which are present in a variety of cells with a primary function of ROS generation.¹⁶ NOX are a family of transmembrane proteins comprising of seven members (namely NOX1, NOX2, NOX3, NOX4, NOX5, DUOX1 and DUOX2).¹⁷ First identified in the kidney,¹⁸ NOX4 is expressed in a wide variety of cells including macrophages¹⁹ and chondrocytes.²⁰ Unlike other NOX isoforms, NOX4 is constitutively active and can produce large quantities of ROS (mainly H₂O₂) when expressed.²¹ Moreover, NOX4, which expression is inducible by well-known proinflammatory cytokines such as IL-1 β ,²² has been identified as a major source of ROS production in chondrocytes.^{20,23,24} Interestingly, injection of advanced oxidation protein products (AOPPs) after anterior cruciate ligament transection (ACLT) in mice increased cartilage damage. Treatment with apocynin, a pan-NOX inhibitor, slowed OA progression. Moreover, after either ACLT or ACLT with AOPPs injection, the expression of NOX4 but not NOX2 or NOX1 was increased.¹⁰ In human chondrocyte cell line, NOX4 regulates MMP-1 expression through ROS generation in response to IL-1 β stimulation.²⁰ Altogether, these results suggest that NOX enzymes, and NOX4 in particular, play a major role in the redox imbalance in OA cartilage.²⁴

The purpose of this study was to determine whether NOX4 contributes to cartilage degradation in a mouse experimental OA model. Using NOX4 KO mice, we observed that NOX4 deficiency protects from cartilage degradation and osteophytes formation after destabilisation of the medial meniscus (DMM). Moreover, NOX4 deletion decreases anabolism and increases catabolism in OA knee cartilage. We also noticed less synovial inflammation, a decrease of ROS production and macrophage recruitment in NOX4 KO mice after DMM. These results suggest that NOX4 could be an interesting therapeutic target to delay cartilage damage in early-stage OA.

MATERIALS AND METHODS

Animals

Mice were bred and housed at the University Medical Center of the University of Geneva. NOX4 knock-out mice (B6.129-Nox4^{tm1Kkr}/J, NOX4^{-/-}) and their wild-type

littermates (WT) were generated as described previously,²⁵ maintained in the C57BL6/J background and used at the age of 10–12 weeks. Only male mice were used to be consistent with previously reported studies on OA research models.²⁶ On day 0, the mice were scanned and underwent DMM. On day 56, the mice were scanned and sacrificed.

Surgery

OA was induced by DMM at day 0 in WT (n=13) and NOX4^{-/-} mice (n=11). DMM was performed on the right knee as previously described,²⁷ while the left contralateral joint underwent a sham surgery. Briefly, mice were anaesthetised using 2% isoflurane, and then maintained under 1% isoflurane during the whole procedure. A 3 cm longitudinal incision was performed over the distal patella to proximal tibial plateau, and the joint was incised and opened with microscissors. Dissection of the fat pad over the intercondylar area was then performed to expose and section the meniscotibial ligament. Buprenorphine (0.05 mg/kg) was provided perioperatively (20 min before surgery) and 4–6 hours after the surgery. Meloxicam (1 mg/kg/day) was administered in drinking water for 3 days. Mice were kept under standard pathogen-free conditions at a constant temperature of 22°C \pm 1°C with a 12-hour light/dark cycle.

Cartilage explant culture

Cartilage explants were obtained from the femoral heads of 10-week-old WT and NOX4^{-/-} mice as described previously.²⁸ The explants were cultured in fetal calf serum (FCS)-free DMEM (Gibco) for 24 hours, then stimulated once with 10 ng/mL of IL-1 β (Preprotech) for 72 hours (n=4 explants per condition). Explants were prepared for cryosectioning followed by immunohistochemistry analysis.

Histological analysis

Mice were sacrificed at day 56. Excised knee joints were fixed in 10% paraformaldehyde, decalcified in EDTA solution for 6 weeks, dehydrated in increasing concentrations of ethanol, and embedded in paraffin. 10 μ m sections from both legs were stained using safranin-O/fast green and examined by light microscopy. The severity of OA was assessed and scored in a blinded manner by three observers. All four quadrants (medial, lateral, tibial and femoral condyles) of the knees were assessed for the final scoring of OA-associated degenerative changes, according to the OA Research Society International (OARSI) system. Cartilage lesions in all four quadrants were scored for OA on a scale from 0 to 6. The average of the worst total score observed by each researcher was used as the OA score for each mouse.^{27,28}

Osteophyte formation was evaluated semi-quantitatively according to a previously described classification system taking into account osteophyte size and maturity²⁹: (0) no formation, (1) cells in the synovial lining stimulated to proliferate, (2) cells inside the developing osteophyte

undergo chondrogenesis and deposit matrix molecules such as aggrecan, (3) the most central chondrocytes further differentiate and hypertrophy, (4) endochondral ossification and formation of marrow cavities and (5) a fully developed osteophyte is integrated with the original subchondral bone and the top of the osteophyte is covered with cartilage expanding the original cartilage surface of the joint.

Synovial inflammation was evaluated using H&E staining. The degree of synovitis was scored as previously reported.²⁸ The thickness of the synovial lining cell layer was evaluated on a scale of 0–3 (0=1–2 cells, 1=2–4 cells, 2=4–9 cells and 3=10 or more cells) and cellular density in the synovial stroma on a scale of 0–3 (0=normal cellularity, 1=slightly increased cellularity, 2=moderately increased cellularity and 3=greatly increased cellularity).

Immunohistochemistry

Immunostaining for COL2 (Abcam), MMP13 (Abcam), 8-hydroxy-2'-deoxyguanosine (8-OHdG, Bioss), type 1 collagen/COL1 (Abcam), NOX4 (Abcam) (Rabbit, 1:100 for each antibody), AGG (Bioss) (Rabbit, 1:50) and F4/80 (Abcam) (Rat, 1:200) was performed on decalcified paraffin-embedded sections of the operated knees. Heat-induced antigen retrieval involved incubation with citrate buffer (pH 6.0) at 80°C for 20 min. Sections were then blocked with peroxidase blocking solution (Dako) for 5 min. Non-specific binding sites were blocked with 5% normal goat serum in 0.3% Triton X100 (Sigma-Aldrich) for 60 min. Primary antibodies were incubated at 4°C overnight. Rabbit (Dako) or rat HRP-conjugated secondary antibodies were incubated for 30 min at room temperature and revealed with the DAB Substrate Kit (Abcam).

To investigate the role of NOX4 and the effect of inflammation on cartilage, untreated and IL-1 β -treated (72 hours) cartilage explants of WT and NOX4^{-/-} mice were fixed with paraformaldehyde, embedded in OCT, and stained with safranin-O or analysed by immunohistochemistry. Cryosectioned slides were subject to immunostaining with the antibodies against COL2, COL1, 8-OHdG, NOX4, AGG and MMP13 (1:200 for each antibody) using the protocol described above. Quantification was performed by manually counting the number of positive staining cells using the FIJI software.

Ex vivo subchondral bone microarchitecture evaluation by micro-CT and histomorphometry

Mice were scanned immediately after sacrifice, at day 56. Right and left lower limbs (for DMM effect assessment) were removed, fixed in paraformaldehyde and dehydrated in ethanol. The tibiae were radiographed using a Quantum Gx micro-CT (Perkin Elmer, voxel 72 μ m³, 360° rotation, rotation step 0.2, scanning time: 15 min (in vivo) or 57 min (ex vivo)), available at the PIPPA (<https://www.unige.ch/medecine/pippa/small-animal-preclinical-imaging-platform/>) facility in Geneva. For analyses, raw data files were imported in another micro-CT (VivaCT40,

Scanco Medical, Bassersdorf, Switzerland) available at the Division of Bone diseases at Geneva Medical University. Three-dimensional reconstructions were generated at the 10.5 μ m cubic resolution and analysed as described previously.³⁰ Three-dimensional structural parameters were obtained from a mean of 21 sections (220.5 μ m) with the following parameters: Sigma: 0.8, Support: 5, Threshold: 131. The area of interest included the region between the articular cartilage and the growth plate. Epiphysal tibia trabecular bone was manually defined by the same operator using Scanco software as illustrated in figure 2B. The following structural parameters of trabecular bone: bone volume fraction (BV/TV, %), trabecular thickness (Tb.Th, μ m), trabecular number (Tb.N, 1/mm), trabecular separation (Tb.Sp, μ m), structure model index (SMI), connectivity density (Conn.D.) were generated. Also, the maximum thickness of the subchondral bone plate (Sb.Th, μ m) was measured on the weight-bearing region at the medial and lateral tibial plateaus.

Bone histomorphometry was performed on histological slides using Bioquant Osteo 19.2.6 software (2018), assessing the following two-dimensional parameters within medial epiphyseal (Ep.) trabecular bone: bone volume fraction (Ep.BV/TV, %), trabecular thickness (Ep.Tb.Th, μ m), trabecular number (Ep.Tb.N, 1/mm), trabecular separation (Ep.Tb.Sp, μ m).

Statistics

Data are reported as mean \pm SE of the mean in the figures. 95% CI, difference in means and eta-square were reported in the text. After verification of Gaussian distribution and homogenous variance of each group, two-way analysis of variance (ANOVA) test or multiple t-test, followed by false discovery rate correction were used to compare experimental conditions. When variance homogeneity was not obtained, the data were transformed using the log function. If variance homogeneity was obtained, we performed a two-way ANOVA test or a multiple t-test followed by false discovery rate correction to compare experimental conditions. Otherwise, a Kruskal-Wallis test with false discovery rate correction was chosen. For in vivo experiments, as sham and DMM surgery were performed on the same mice, we used the RM-two ways ANOVA. The significance level was set at $p < 0.05$. GraphPad Prism V.8.0 (San Diego, California, USA) was used for analysis.

RESULTS

Whole body NOX4 deletion reduces cartilage degradation after DMM

We induced experimental OA by DMM in WT and NOX4^{-/-} mice and we evaluated OA at day 56 post injury. We observed large areas of cartilage erosion (around 50% of the cartilage width) indicating mild to severe OA developed after 8 weeks in WT mice. In NOX4^{-/-} mice, cartilage damage was less extensive with only small fibrillations and occasional loss of cartilage staining (figure 1A). Using the OARSI scoring system,

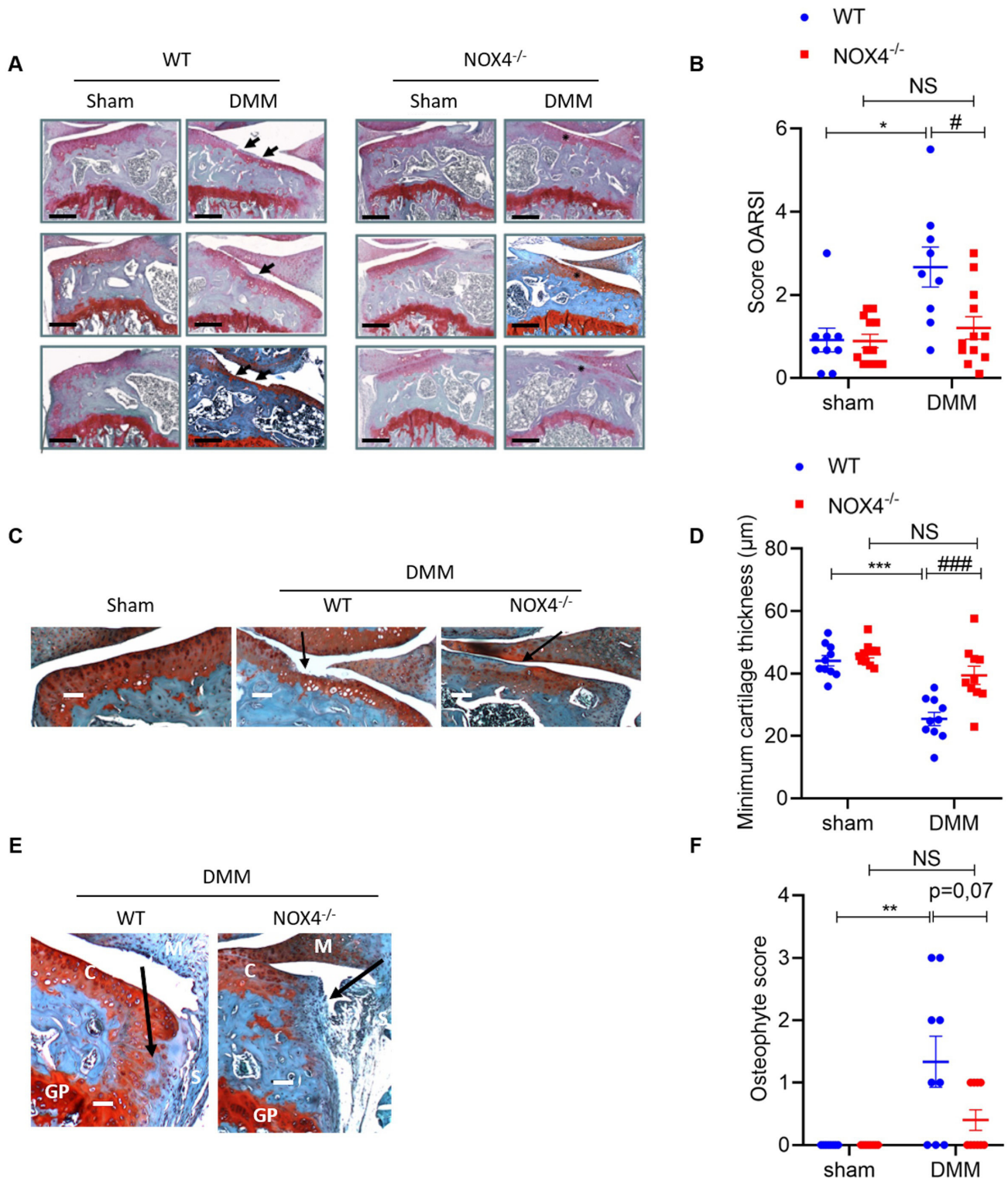


Figure 1 Deletion of NOX4 reduces cartilage degradation. (A) Knee sections stained with safranin-O from NOX4^{-/-} (n=13 mice) and WT (n=11 mice). Cartilage lesions are shown with a black arrow. Scale bars: 250 μm. (B) OA lesions were assessed by OARSI score. RM-Two ways ANOVA on log transformed data test with FDR correction between WT and NOX4^{-/-} (#) or between Sham and DMM (*). *p<0.05, **p<0.01, ***p<0.001. (C) Representative images of the minimum cartilage thickness and (D) its quantification using the Zen software (n=10). RM-Two ways ANOVA test with FDR correction between WT and NOX4^{-/-} (#) or between Sham and DMM (*). *p<0.05, **p<0.01, ***p<0.001. Scale bars: 200 μm. (E) Representative images of osteophytes formation after DMM (M: meniscus, S: synovial membrane, C: cartilage and GP: growth plate). Osteophytes are showed with a black arrow. Scale bars: 200 μm. (F) Osteophytes formation were quantified with the osteophyte score (n=9). Kruskal-Wallis test with FDR correction between WT and NOX4^{-/-} (#) or between sham and DMM (*). *p<0.05, **p<0.01, ***p<0.001. ANOVA, analysis of variance; FDR, false discovery rate; DMM, destabilisation of the medial meniscus; OARSI, OA Research Society International.

we assessed the OA grade as 2.467 ± 0.473 in WT mice vs 1.103 ± 0.266 ($p=0.0139$, 95% CI 0.28 to 0.76, difference in means=1.48 and $\eta^2=10.24$) in NOX4^{-/-} mice (figure 1B). We also measured cartilage thickness on safranin-O-stained sections (figure 1C). After DMM, we observed a minimum cartilage thickness of $25.417 \mu\text{m} \pm 2.12$ in WT mice vs $39.414 \mu\text{m} \pm 2.965$ ($p<0.0001$, 95% CI 8.52 to 16.86, difference in means=12.69 and $\eta^2=15.44$) in NOX4^{-/-} mice (figure 1D). Lastly, we evaluated, on safranin-O-stained sections, the formation of osteophytes at the medial part of the joints (figure 1E). We observed that the osteophyte score was of 1.33 ± 0.41 in WT vs 0.4 ± 0.16 ($p=0.07$, 95% CI 0.63 to 1.00, difference in means=0.47) in NOX4^{-/-} (figure 1F).

These results indicate that whole body deletion of NOX4 protects from OA severity and cartilage degradation after DMM.

Ex vivo subchondral bone microarchitecture evaluation by micro-CT and histomorphometry

Progression and severity of OA is associated with modifications of the subchondral bone. We therefore measured the thickness of the subchondral bone and total epiphyseal bone parameters by three-dimensional micro-CT. DMM induced pronounced sclerosis of the subchondral bone at the medial plateau in both WT and NOX4^{-/-} mice (figure 2A,B). At the lateral tibial plateau, neither WT nor NOX4^{-/-} mice showed an increase of subchondral bone thickness after DMM, which was also comparable to that of unoperated knees (figure 2B). As compared with sham knees, DMM slightly increased total epiphyseal BV/TV and Tb.Th in WT mice (+13% and +2.9%, respectively; table 1), as well as in NOX4^{-/-} mice (+2.3% and +3.80%, respectively) but these increases did not reach significance. Interestingly, whereas trabecular Conn.D was significantly reduced in WT mice (-30% vs sham; $p=0.001$; table 1), it was not significantly altered in NOX4^{-/-} mice (-9.5% vs sham; $p=0.296$; table 1).

We also analysed bone architecture using bone histomorphometry. Qualitative observations of safranin-O-stained sections revealed that densification was more important in the medial than in the lateral part of the subchondral bone (figure 2C). As the surgery was performed on the medial meniscus, we decided to measure the subchondral bone parameters specifically in the medial area. As observed using micro-CT analysis, DMM increased BV/TV and Tb.Th in the medial part of the epiphysis in WT mice, as compared with sham knees (+37% and +102%, $p=0.003$, 95% CI -15.71 to -5.53, difference in means=-10.62 and $\eta^2=16.05$; and $p=0.0187$, 95% CI -137.7 to -18.83, difference in means=-78.28 and $\eta^2=14.89$). Of note, DMM failed to significantly increase these parameters in NOX4^{-/-} mice (+21% and +46%, $p=0.0961$, 95% CI -8.90 to 9.38, difference in means=0.24 and $\eta^2=0.01$; and $p=0.0951$, 95% CI -44.27 to 70.15, difference in means=12.94 and $\eta^2=0.44$) (figure 2D).

Overall, these data suggested that DMM induced significant alterations in WT subchondral bone whereas these modifications were less pronounced in NOX4^{-/-} mice.

Deletion of NOX4 rescues the anabolic/catabolic balance

To investigate the effect of NOX4 on the anabolic and catabolic activity of the cartilage, we studied the expression of anabolic markers (COL2 and AGG) and catabolic markers (COL1 and MMP13) in WT and NOX4^{-/-} knee joints following DMM.

We observed a significant decrease of COL2 and AGG staining in DMM knee joints (respectively, $37.1 \pm 4.4\%$ and $28.2 \pm 3.3\%$) of WT mice as compared with sham knee joints (respectively, $92.6 \pm 0.6\%$ and $80.7 \pm 4.3\%$) of WT mice (COL2: 95% CI 30.27 to 41.361, difference in means=35.81 and $\eta^2=59.23$ and AGG: 95% CI 22.87 to 34.93, difference in means=28.90 and $\eta^2=34.90$). Interestingly, we noticed that immunostaining for COL2 and AGG in DMM knee joints of NOX4^{-/-} (respectively, $76.2 \pm 1.9\%$ and $80.5 \pm 1.6\%$) mice was higher than in DMM knee joints (respectively, $37.1 \pm 4.4\%$ and $28.2 \pm 3.3\%$) of WT mice (COL2: 95% CI -24.78 to -13.87, difference in means=-19.32 and $\eta^2=17.24$ and AGG: 95% CI -35.93 to -21.31, difference in means=-28.62 and $\eta^2=34.22$) (figure 3A,B).

We also evaluated COL1 expression, a marker of chondrocytes dedifferentiation, in WT and NOX4^{-/-} mice after DMM. In WT mice, we observed that DMM induced a strong increase of COL1 expression ($58.9 \pm 6.3\%$ vs $15.7 \pm 2.3\%$, 95% CI -40.44 to -20.87, difference in means=-30.66 and $\eta^2=58.10$). In comparison, we observed very few COL1-positive cells in the NOX4^{-/-} DMM mice ($33.6 \pm 4.2\%$, 95% CI 3.77 to 21.84, difference in means=12.81 and $\eta^2=10.14$) (figure 3A,B).

Finally, we assessed cartilage catabolism through MMP13 immunostaining. We observed that MMP13 expression was significantly upregulated in DMM knee joints of WT mice as compared with sham knee joints ($67.1 \pm 4.6\%$ vs $41.9 \pm 2.7\%$, 95% CI -39.83 to -32.37, difference in means=-36.10 and $\eta^2=69.72$). Interestingly, the number of MMP13 positive cells was lower in NOX4^{-/-} DMM knee joints as compared with WT ($41.9 \pm 2.7\%$ vs $67.1 \pm 4.6\%$, 95% CI 4.19 to 24.75, difference in means=14.47 and $\eta^2=11.20$) (figure 3A,B).

These results indicate that NOX4 deletion restores the metabolic balance by upregulating anabolism and down-regulating catabolism.

Deletion of NOX4 protects cartilage from degradation in an IL-1 β -induced OA model

We collected femoral heads from WT and NOX4^{-/-} mice and induced an OA-like phenotype by stimulating cartilage explants with IL-1 β (10 ng/mL) for 72 hours.

In WT explants, IL-1 β induced loss of proteoglycans from the superficial zone of the cartilage in safranin-O-stained sections (figure 4A). We also observed a decrease of AGG expression and an increase of MMP13 and COL1 expression, but no changes in COL2 expression.

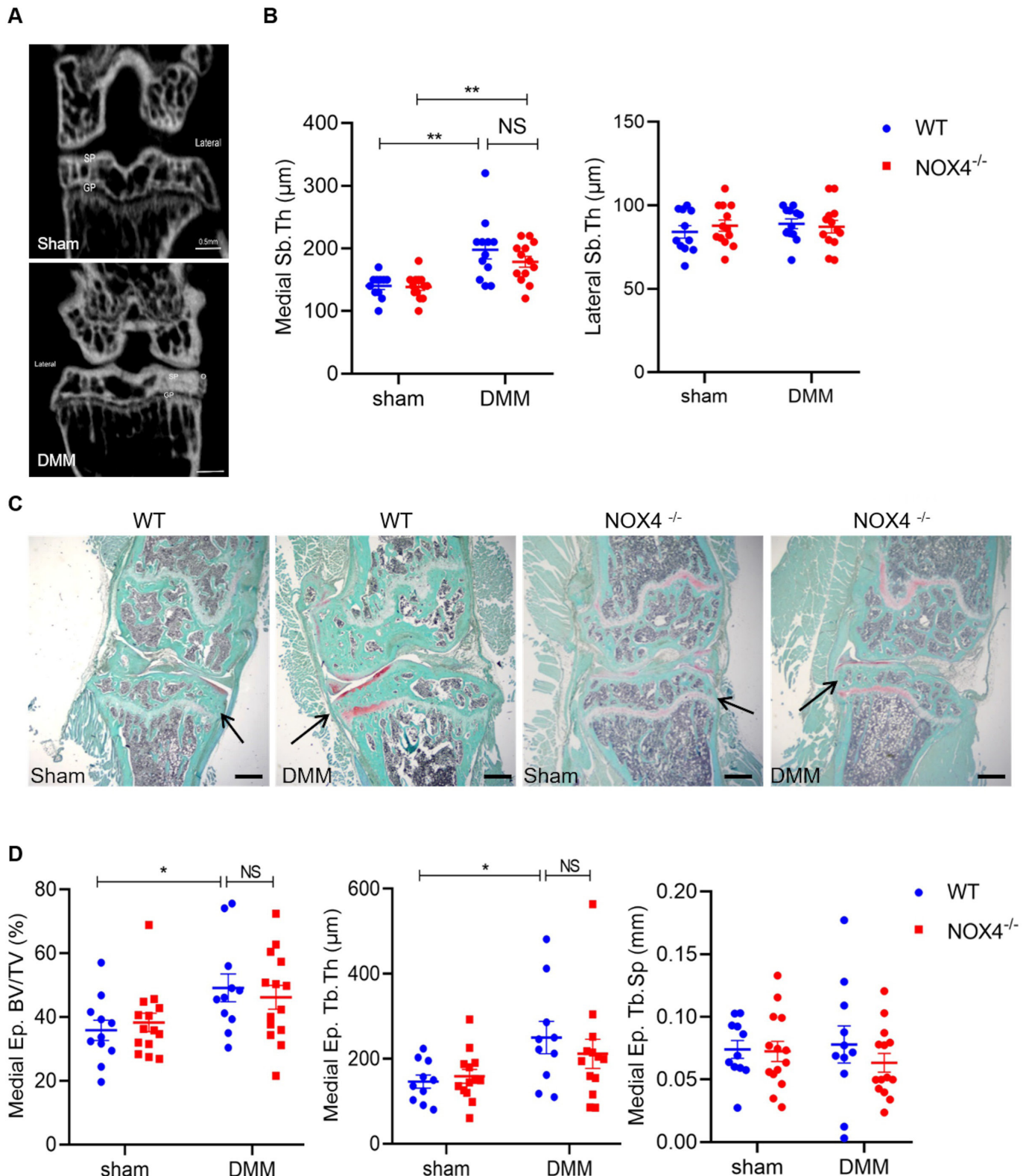


Figure 2 Ex vivo subchondral bone microarchitecture evaluation by micro-CT and histomorphometry. (A) Micro-CT images of a WT sham and DMM knee 8 weeks after DMM (SP: subchondral plate, GP: growth plate and O: osteophyte). (B) Quantification of the maximum Sb.Th of the lateral and medial part of the knee (WT: N=11 and NOX4^{-/-}: N=13). (C) Representative images of the safranin-safranin-O stained sections used for histomorphometry. Black arrow shows the medial part of the joint. Scale bars: 250 µm. (D) Quantification of the different subchondral bone parameters on the medial part of the epiphysis: BV/TV, Tb.Th and Tb.Sp (WT: N=11 and NOX4^{-/-}: N=13). RM-two-way ANOVA test on log transformed data with FDR correction between WT and NOX4^{-/-} (#) or between sham and DMM (*). *p<0.05, **p<0.01, ***p<0.001. ANOVA, analysis of variance; DMM, destabilisation of the medial meniscus; FDR, false discovery rate; WT, wild type.

Table 1 Effect of surgery on epiphyseal tibial trabecular microarchitecture in WT and NOX4^{-/-} mice

Parameters	NOX4 ^{+/+}				NOX4 ^{-/-}				Pairwise comparisons							
	Genotype		DMM		Sham		DMM		Two-way ANOVA		DMM effect		NOX4 ^{-/-}			
	Abbreviation	Mean	SE	Mean	SE	Mean	SE	Mean	SE	Genotype Effect	DMM Effect	Int	% of r	p	% of r	p
Tibia trabecular epiphyseal bone	Bone volume fraction	42.19	3.77	47.68	3.66	46.94	2.94	48.02	2.96	0.449	0.331	0.511	13.01	0.318	2.30	0.800
	Trabecular number	7.65	0.14	7.63	0.19	7.55	0.17	7.29	0.11	0.169	0.370	0.435	-0.26	0.938	-3.44	0.216
	Trabecular separation	96.0	5.1	95.6	5.3	95.4	3.1	92.9	3.6	0.696	0.724	0.807	-0.49	0.950	-2.66	0.597
	Trabecular thickness	139.6	1.9	143.6	5.1	140.5	3.2	145.9	3.6	0.658	0.195	0.859	2.90	0.448	3.80	0.284
	Connectivity density	104.8	5.6	73.2	5.2	100.1	7.7	90.7	4.3	0.291	0.002	0.074	-30.16	0.001	-9.45	0.296
	Structure model index	0.850	0.330	-0.050	0.390	0.220	0.310	0.260	0.250	0.633	0.187	0.150	-105.88	0.099	18.18	0.920
	Tissue mineral density	4837	29	4823	24	4785	23	4790	26	0.112	0.872	0.711	-0.29	0.723	0.11	0.877

Significant p values are marked in bold. ANOVA, analysis of variance; DMM, destabilisation of the medial meniscus.

In comparison to WT, the IL-1 β -treated NOX4^{-/-} cartilage had higher expression of AGG (85.6% \pm 1.4% vs 40.7% \pm 5.3%, 95% CI -29.69 to -15.00, difference in means=-22.34 and $\eta^2=31.90$), lower expression of MMP13 (40.8% \pm 3.5% vs 86% \pm 0.8%, 95% CI 17.22 to 30.51, difference in means=23.87 and $\eta^2=23.31$) and COL1 (28.8% \pm 2.8% vs 69.9% \pm 5.2%, 95% CI -35.45 to -17.04, difference in means=20.82 and $\eta^2=39.44$) and a higher proteoglycan content in the superficial zone of the cartilage (figure 4A,C).

Many studies have suggested that increased oxidative stress could be the cause of metabolism perturbations in chondrocytes.³¹ As the main function of NOX4 is to produce H₂O₂, we performed immunohistochemistry experiments with an antibody against NOX4 or against 8-OHdG (marker of ROS) antibodies (figure 4B). We observed increased expression of NOX4 in WT explants treated with IL-1 β (59.6% \pm 7.5% vs 21.8% \pm 5.2%, 95% CI -28.84 to -8.96, difference in means=-18.90 and $\eta^2=13.62$). In addition, IL-1 β stimulation increased cartilage expression of 8-OHdG in WT but not in NOX4^{-/-} explants (65% \pm 3.2% vs 25.2% \pm 1.5%, 95% CI 18.34 to 30.60, difference in means=24.47 and $\eta^2=39.36$) (figure 4C).

These data demonstrate that the treatment with IL-1 β disrupted the anabolic-catabolic balance in the cartilage, upregulated NOX4 expression and induced oxidative stress. NOX4 deletion restored the metabolic balance and prevented ROS production.

Deletion of NOX4 protects from cartilage degradation and inflammation via inhibition of oxidative stress

One of the main factors associated with the progression of OA is low-grade inflammation,⁶ and oxidative stress is known to induce inflammation. We, therefore, assessed the impact of NOX4 deletion on inflammation and oxidative stress.

First, using H&E staining, we demonstrated that DMM induces synovial inflammation (increased cellularity and thickness) in WT but not in NOX4^{-/-} mice (figure 5A). WT mice had higher synovitis score than NOX4^{-/-} mice (2.5 \pm 0.5 vs 0.9 \pm 0.4, respectively; p=0.006, 95% CI 0.001 to 1.60, difference in means=0.80 and $\eta^2=12.08$) (figure 5B). In line with these results, we observed a strong decrease of F4/80 expression, a well-known macrophage marker, in the synovial membranes of NOX4^{-/-} mice as compared with WT mice (figure 5C).

We evaluated the expression of NOX4 by immunohistochemistry. We observed that DMM induced NOX4 expression in the cartilage (52.9% \pm 5.5% vs 13.5% \pm 1.8%, 95% CI 24.70 to 54.16, difference in means=39.43) but not in the synovial membrane or the meniscus (figure 5D,E).

Finally, we assessed the effect of NOX4 deletion on oxidative stress. We observed less 8-OHdG staining in the cartilage of NOX4^{-/-} mice after DMM as compared with the WT mice (12.9% \pm 2.3% vs 67.5% \pm 2.6%, 95% CI 26.48 to 34.23, difference in means=30.36 and $\eta^2=39.70$) (figure 5C,E).

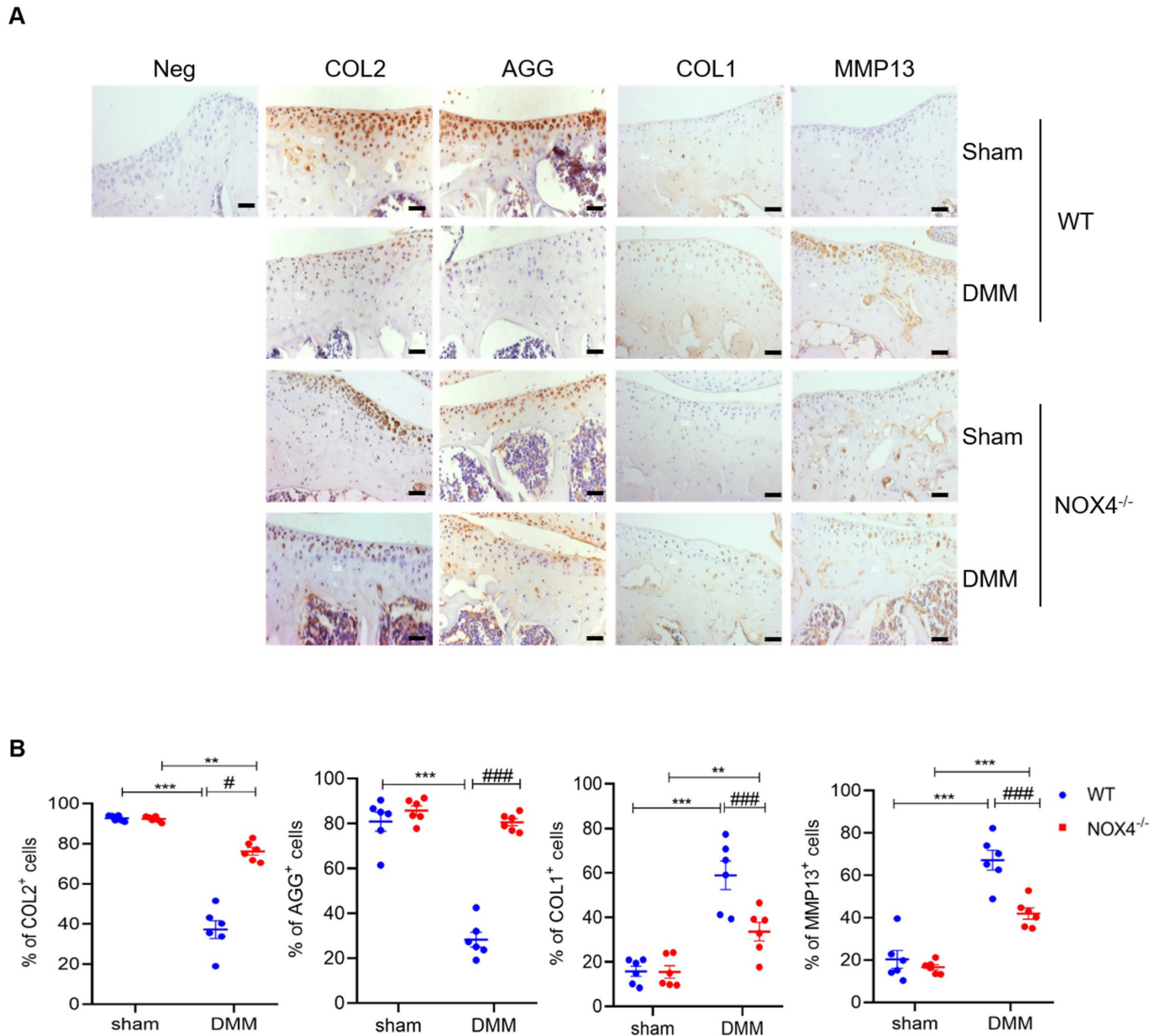


Figure 3 Deletion of NOX4 rescues the anabolic/catabolic balance. A) Representative IHC images of knee cartilage sections stained with COL2, AGG, COL1 and MMP13 antibody (N=6). Please note that DMM decreased AGG and COL2 expression and increase MMP13 and COL1 expression in the cartilage of WT mice but not in NOX4^{-/-}. Scale bars: 40 μm. (B) Quantification of the proportions of positive cells for COL2, AGG, COL1 and MMP13 staining in the superficial cartilage. RM-two-way ANOVA test with FDR correction between WT and NOX4^{-/-} (#) or between sham and DMM (*). *p<0.05, **p<0.01, ***p<0.001. ANOVA, analysis of variance; DMM, destabilisation of the medial meniscus; FDR, false discovery rate; WT, wild type. IHC: Immunohistochemistry.

Taken together, these results prove that NOX4 is necessary for oxidative stress and inflammation during OA.

DISCUSSION

NOX family is suspected to be a major contributor of oxidative stress in the osteoarthritic joints through the production of ROS.^{15,32} Using a model of joint instability, we demonstrated that NOX4 deficiency reduces OA severity and that NOX4 plays a major role in joint inflammation, cartilage metabolism and oxidative stress.

The DMM model that has been used in the present study induces in 6–8 weeks moderate to severe OA which resembles human OA.^{25,32} Importantly, surgically induced changes following DMM are comparable to those occurring naturally in mice with ageing, and are most severe in the medial compartment.²⁶ We performed DMM in male mice to be consistent with the vast majority of previously published studies, although similar progression of disease has been reported in male and female mice using this model.³³

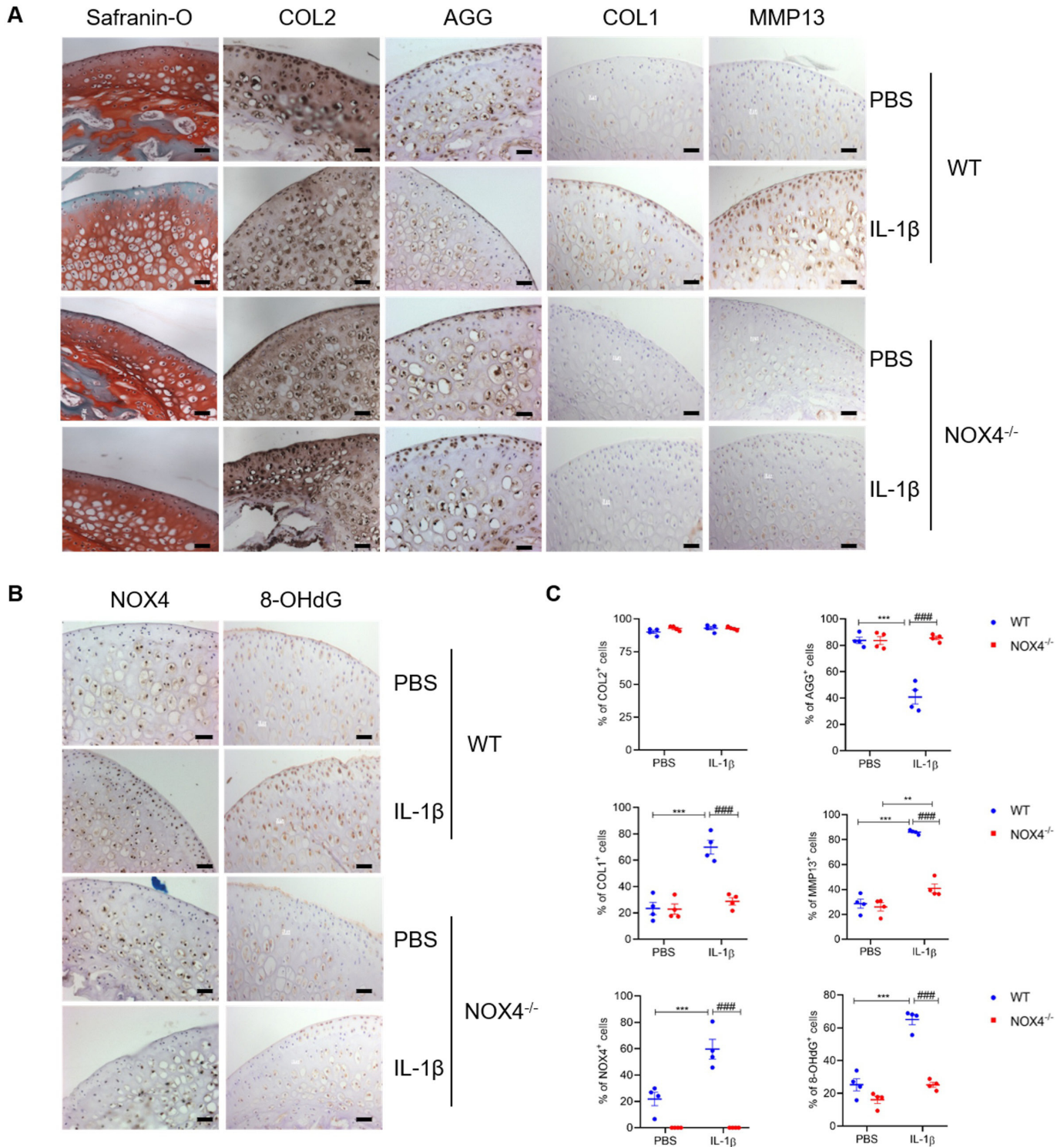


Figure 4 Deletion of NOX4 protects cartilage in an IL-1 β -induced osteoarthritis (OA) model. (A) Representative images of femoral heads explants, safranin-O staining and IHC of anabolism (COL2 and AGG) and catabolism (MMP13 and COL1). (B) NOX4 and 8-OHdG IHC. Please note that IL-1 β treatment decreased AGG expression and increased MMP13 and COL1 expression in the cartilage of WT explants but not in NOX4^{-/-}. Scale bars: 40 μ m. (C) Quantification of the proportions of positive cells for COL2, AGG, COL1, MMP13, NOX4 and 8-OHdG staining in the superficial cartilage. RM-two-way ANOVA test with FDR correction between WT and NOX4^{-/-} (#) or between sham and DMM (*). * $p < 0.05$, ** $p < 0.01$, *** $p < 0.001$. ANOVA, analysis of variance; WT, wild type. IHC: Immunohistochemistry.

OA is primarily driven by enhanced catabolic activity, accelerated dedifferentiation of chondrocytes, high ROS production, and low anabolic activity in response

to biomechanical and inflammatory stimuli. In this study, we demonstrated for the first time that NOX4 deletion reduces OA severity in an in vivo model. As

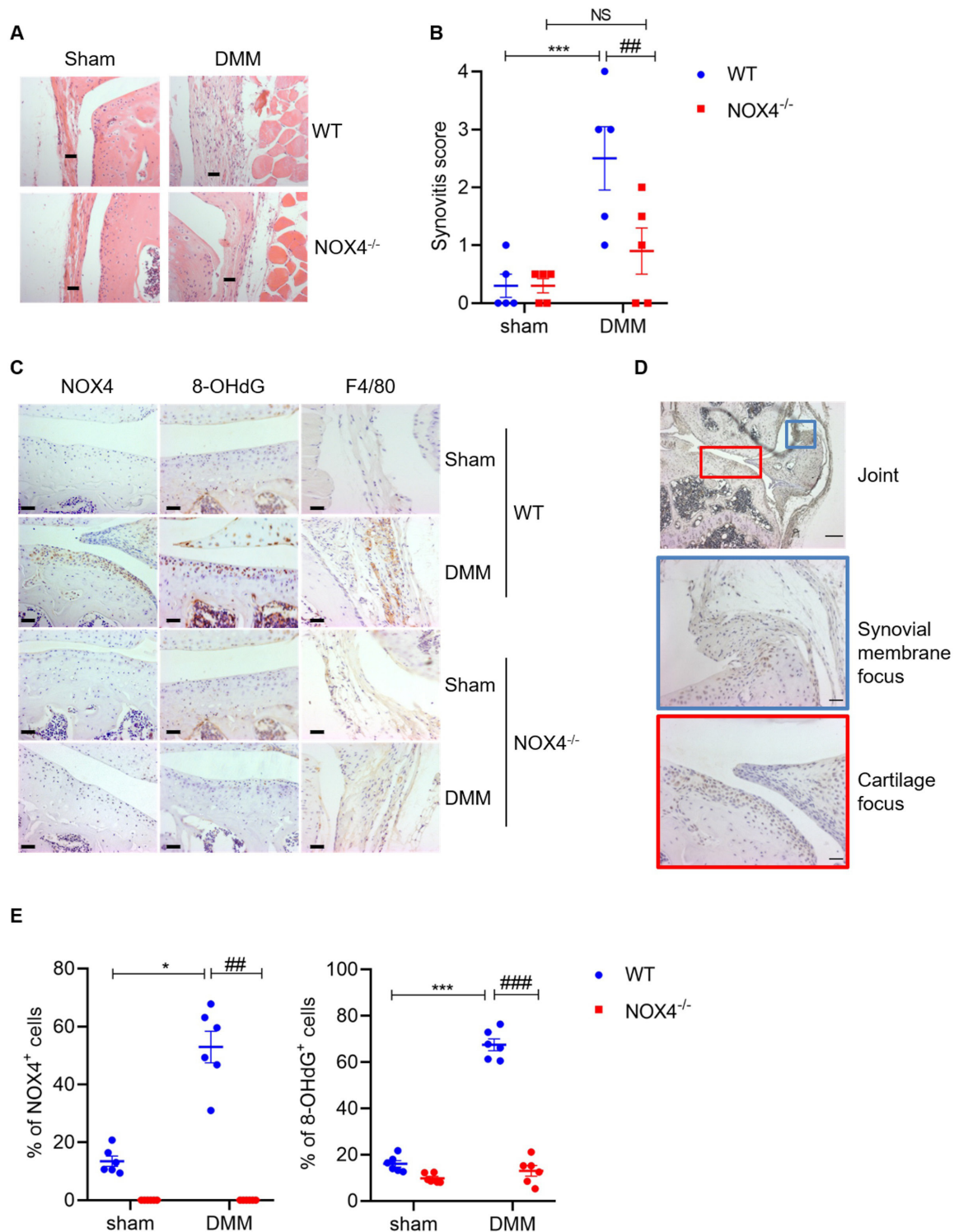


Figure 5 Deletion of NOX4 protects from cartilage degradation and inflammation via inhibition of oxidative stress. (A) Knee sections focus on synovial membrane stained with H&E from NOX4^{-/-} and WT (n=5 mice). Scale bars: 20 μ m. (B) Quantification of the synovial inflammation using the synovitis score. RM-two-way ANOVA test with FDR correction between WT and NOX4^{-/-} (#) or between sham and DMM (*). (C) Representative IHC images of knee sections stained with NOX4, 8-OHdG and F4/80 antibody (N=6). Please note that DMM increased NOX4, 8OHdG and F4/80 expression in WT mice. There was no expression of 8OHdG and F4/80 in the NOX4^{-/-} mice. Scale bars: 40 μ m. (D) Representative IHC image of the whole Knee stained with NOX4 antibody (scale bar: 200 μ m) and a focus on the synovial membrane (blue rectangle, scale bar: 40 μ m) and the cartilage (red rectangle, scale bar: 40 μ m). We observed an expression of NOX4 in the cartilage (red rectangle) and not the synovial membrane (blue rectangle) of the joints. (E) Quantification of the proportions of positive cells for NOX4 and 8-OHdG staining in the superficial cartilage. RM-two ways ANOVA test with FDR correction between WT and NOX4^{-/-} (#) or between Sham and DMM (*). *p<0.05, **p<0.01, ***p<0.001. ANOVA, analysis of variance; DMM, destabilisation of the medial meniscus; FDR, false discovery rate; WT, wild type. IHC: Immunohistochemistry.

compared with WT knees, our data show that NOX4 deletion significantly reduces cartilage degradation, osteophyte formation and synovial inflammation. In a non-invasive OA model resulting from ACL rupture, Wegner *et al*³⁴ observed a sustained low level of increased NOX4 expression during the first 2–7 days after injury, and demonstrated that inhibition of NOX4 activity was protective against early structural changes evaluated in the subchondral bone at 7 days. In line with preceding studies using *in vitro* cultures of chondrocytes,^{20 22 23} we observed that NOX4 is a major component for the expression of MMP and ROS production in mouse cartilage. In OA, it is well known that low-grade inflammation in the synovium plays a major role in the progression of the disease.^{1 6} In WT but not in the NOX4^{-/-} mice, increased cellularity and thickness of the synovium was observed, together with an increased expression of the macrophage marker F4/80. Taken together, our results demonstrate that NOX4 is a major player involved in the perturbation of joint homeostasis in OA. Another NOX isoform has been also reported to play an important role in cartilage homeostasis. In a collagenase-induced OA model in mice, NOX2 deficiency reduced cartilage damage, synovium thickness and ectopic bone formation at day 21.³⁵ In the mice synovium, NOX2 is mainly expressed by M2-like macrophages, and could play an important role in subtypes of OA characterised by synovial inflammation.

Subchondral bone plate modifications occur early in the development of OA, prior to trabeculae modifications, and ahead of microscopic cartilage degeneration.³⁶ In line with previously reported studies,²⁶ sclerosis of the subchondral bone plate was found at 8 weeks following DMM at the medial side of the tibial plateau. These findings were observed in both WT and NOX4^{-/-} mice and were located where the amount of cartilage damage was most important in the load-bearing area. No changes were observed at the lateral side of the epiphysis with a subchondral plate thickness that was comparable to that of non-operated knees. Interestingly, the DMM procedure also affected the trabecular subchondral bone structure in the medial epiphysis with an increase of both the BV/TV and Tb.Th in WT mice, while these parameters were not significantly increased in NOX4^{-/-} mice when analysed by histomorphometry. Also, the connectivity density, which characterises the redundancy of trabecular connections was significantly reduced in WT mice, but not in NOX4^{-/-} mice. Increased number and thickness of trabeculae and decreased connectivity density are indicative of advanced OA, as reported in several studies.^{37 38} To our knowledge, only one study has evaluated the effect of NOX4 deletion on the underlying bone in a post-traumatic model of OA,³⁴ but this was performed at an early stage after OA induction. At 7 days, WT and NOX4^{-/-} mice had a statistically significant decrease in subchondral bone density, while injured knees from WT mice treated with NOX4 inhibitor did not. Recently, a growing number of studies have pointed out the role of the subchondral bone in OA

pathogenesis. Among the different metabolic pathways involved, PI3K/AKT/mTOR signalling pathway has been shown to play a key role, as it increases bony sclerosis and cartilage degradation following DMM, through the activation of NF- κ B pathway a potent inducer of MMP-13 expression.³⁹ As reported in cancer research studies,^{40 41} NOX4 could also exacerbate OA through inhibition of AMPK and activation of PI3K/AKT/mTOR signalling, but this was not tested in our study.

Oxidative stress induces inflammation in numerous cell types including chondrocytes and macrophages.^{8 10 42–44} AOPPs induce IL-1 β and TNF- α secretion in chondrocytes. Moreover, AOPPs injection in mice knee induces cartilage degradation and inflammatory cytokines production.¹⁰ In patients, OA severity correlates with AOPPs concentration in the synovial fluid.¹⁰ In our study, we report an increase of oxidative stress (8-OHdG) in cartilage and synovial membrane 8 weeks after DMM in WT mice, a phenomenon which was significantly reduced in NOX4^{-/-} mice. Oxidative stress inhibition in NOX4^{-/-} knee is also associated with an attenuation of the inflammatory response (macrophages) after DMM. These results support the predominant role of ROS observed in other OA models^{14 45–47} and suggest that the excess production of H₂O₂ by NOX4 following joint destabilisation could determine the progression of OA. It is possible that the mechanical stress caused by destabilisation of the joints increases NOX4 activity inducing ROS production and oxidative stress, which, in turn, leads to macrophages recruitment. Other *in vitro* studies have shown that shear stress induces NOX4-dependent ROS production in several cell types.^{48 49} However, the link between mechanical stress and NOX4 in OA requires further investigation.

Our data demonstrated that in mice the deletion of NOX4 could delay the progression of OA. Still, the relevance of our data in the clinical setting is unclear. Few previous studies have evaluated the impact of NOX4 in human joints and bone diseases. *In vitro*, it was demonstrated that treatment of human chondrocytes with IL-1 β increases the expression NOX4 and of the catabolic markers MMP1, MMP13 and ADAMTS4. Moreover, the treatment of human chondrocytes with different NOX inhibitors strongly inhibits ROS production and MMP1 and MMP13 expression.²² On sections of human cartilage extracted from patients undergoing knee replacement surgery, it was shown that NOX4 staining was higher in the damaged sections as compared with the healthy areas. Interestingly, in osteoporosis, it was demonstrated that patients with the NOX4 SNP rs11018628 had a higher NOX4 gene expression. Also, osteoclast activity and bone turnover were increased and women with this SNP had a lower bone density.⁵⁰ Densification of the subchondral bone is known to play a role in OA. It would be interesting to see if patients with the NOX4 rs11018628 SNP developed more severe OA. Moreover, NOX4 has been demonstrated to be necessary for human osteoclast differentiation.⁵⁰ The precursors of the osteoclast lineage

are the macrophages, which suggests that NOX4 could directly impact the macrophages, one of the cell type responsible for the inflammatory response in OA.

Overall, our results provide evidence that NOX4 play a central role in the pathogenesis of OA. Whole body deletion of NOX4 restores cartilage homeostasis, inhibits oxidative stress and inflammation and delays OA progression after DMM in mice. These findings can help identify new targets for OA treatment.

Acknowledgements We thank Didier Colin for providing access to the Small Animal Preclinical Imaging Platform, Beata Kusmider for valuable comments on the manuscript, and Cyril Jaksic for advice on statistical analysis.

Contributors FR and KO contributed equally to the manuscript. All authors were involved in drafting the article or revising it critically for important intellectual content, and all authors approved the final version to be published. FR and KO have full access to all of the data in the study and take responsibility for the integrity of the data and the accuracy of the data analysis. DH acts as guarantor for the study.

Funding This study was supported by a research grant from the Department of Orthopaedic Surgery, Geneva University Hospitals, Geneva, Switzerland.

Competing interests None declared.

Patient consent for publication Not applicable.

Ethics approval Experiments were performed in compliance with the institutional guidelines and following protocols approved by the Ethical Committee on Use and Care of Animals (authorisation GE/05/17).

Provenance and peer review Not commissioned; externally peer reviewed.

Data availability statement Data sharing not applicable as no datasets generated and/or analysed for this study.

Open access This is an open access article distributed in accordance with the Creative Commons Attribution Non Commercial (CC BY-NC 4.0) license, which permits others to distribute, remix, adapt, build upon this work non-commercially, and license their derivative works on different terms, provided the original work is properly cited, appropriate credit is given, any changes made indicated, and the use is non-commercial. See: <http://creativecommons.org/licenses/by-nc/4.0/>.

ORCID ID

Félix Renaudin <http://orcid.org/0000-0002-5712-582X>

REFERENCES

- Berenbaum F. Osteoarthritis as an inflammatory disease (osteoarthritis is not osteoarthrosis!). *Osteoarthritis Cartilage* 2013;21:16–21.
- Bijlsma JWJ, Berenbaum F, Lefeber FJG. Osteoarthritis: an update with relevance for clinical practice. *Lancet* 2011;377:2115–26.
- Carr AJ, Robertsson O, Graves S, et al. Knee replacement. *Lancet* 2012;379:1331–40.
- Lohmander LS, Dahlberg L, Eyre D, et al. Longitudinal and cross-sectional variability in markers of joint metabolism in patients with knee pain and articular cartilage abnormalities. *Osteoarthritis Cartilage* 1998;6:351–61.
- Nam J, Perera P, Liu J, et al. Sequential alterations in catabolic and anabolic gene expression parallel pathological changes during progression of monoiodoacetate-induced arthritis. *PLOS ONE* 2011;6:e24320.
- Robinson WH, Lepus CM, Wang Q, et al. Low-Grade inflammation as a key mediator of the pathogenesis of osteoarthritis. *Nat Rev Rheumatol* 2016;12:580–92.
- Mittal M, Siddiqui MR, Tran K, et al. Reactive oxygen species in inflammation and tissue injury. *Antioxid Redox Signal* 2014;20:1126–67.
- Liu L, Luo P, Yang M, et al. The role of oxidative stress in the development of knee osteoarthritis: a comprehensive research review. *Front Mol Biosci* 2022;9:1001212.
- Martin G, Andriamanalijaona R, Mathy-Hartert M, et al. Comparative effects of IL-1beta and hydrogen peroxide (H2O2) on catabolic and anabolic gene expression in juvenile bovine chondrocytes. *Osteoarthritis Cartilage* 2005;13:915–24.
- Liao C-R, Wang S-N, Zhu S-Y, et al. Advanced oxidation protein products increase TNF- α and IL-1 β expression in chondrocytes via NADPH oxidase 4 and accelerate cartilage degeneration in osteoarthritis progression. *Redox Biol* 2020;28:101306.
- Henrotin Y, Kurz B, Aigner T. Oxygen and reactive oxygen species in cartilage degradation: friends or foes? *Osteoarthritis Cartilage* 2005;13:643–54.
- Koike M, Nojiri H, Ozawa Y, et al. Mechanical overloading causes mitochondrial superoxide and SOD2 imbalance in chondrocytes resulting in cartilage degeneration. *Sci Rep* 2015;5:11722.
- Zhu S, Makosa D, Miller B, et al. Glutathione as a mediator of cartilage oxidative stress resistance and resilience during aging and osteoarthritis. *Connect Tissue Res* 2020;61:34–47.
- Kaneko Y, Tanigawa N, Sato Y, et al. Oral administration of N-acetyl cysteine prevents osteoarthritis development and progression in a rat model. *Sci Rep* 2019;9:18741.
- Tudorachi NB, Totu EE, Fifea A, et al. The implication of reactive oxygen species and antioxidants in knee osteoarthritis. *Antioxidants (Basel)* 2021;10:985.
- Bedard K, Krause KH. The Nox family of ROS-generating NADPH oxidases: physiology and pathophysiology. *Physiol Rev* 2007;87:245–313.
- Lambeth JD. Nox enzymes and the biology of reactive oxygen. *Nat Rev Immunol* 2004;4:181–9.
- Geiszt M, Kopp JB, Várnai P, et al. Identification of renox, an NAD (P) H oxidase in kidney. *Proc Natl Acad Sci U S A* 2000;97:8010–4.
- Lee CF, Qiao M, Schröder K, et al. Nox4 is a novel inducible source of reactive oxygen species in monocytes and macrophages and mediates oxidized low density lipoprotein-induced macrophage death. *Circ Res* 2010;106:1489–97.
- Grange L, Nguyen MVC, Lardy B, et al. Nad (P) H oxidase activity of Nox4 in chondrocytes is both inducible and involved in collagenase expression. *Antioxid Redox Signal* 2006;8:1485–96.
- Martyn KD, Frederick LM, von Loehneysen K, et al. Functional analysis of Nox4 reveals unique characteristics compared to other NADPH oxidases. *Cell Signal* 2006;18:69–82.
- Rousset F, Hazane-Puch F, Pinosa C, et al. IL-1beta mediates MMP secretion and IL-1beta neosynthesis via upregulation of P22 (phox) and nox4 activity in human articular chondrocytes. *Osteoarthritis Cartilage* 2015;23:1972–80.
- Kim KS, Choi HW, Yoon HE, et al. Reactive oxygen species generated by NADPH oxidase 2 and 4 are required for chondrogenic differentiation. *J Biol Chem* 2010;285:40294–302.
- Drevet S, Gavazzi G, Grange L, et al. Reactive oxygen species and NADPH oxidase 4 involvement in osteoarthritis. *Exp Gerontol* 2018;111:107–17.
- Carnesecchi S, Deffert C, Donati Y, et al. A key role for Nox4 in epithelial cell death during development of lung fibrosis. *Antioxid Redox Signal* 2011;15:607–19.
- McNulty MA, Loeser RF, Davey C, et al. Histopathology of naturally occurring and surgically induced osteoarthritis in mice. *Osteoarthritis Cartilage* 2012;20:949–56.
- Glasson SS, Blanchet TJ, Morris EA. The surgical destabilization of the medial meniscus (DMM) model of osteoarthritis in the 129/svev mouse. *Osteoarthritis Cartilage* 2007;15:1061–9.
- Latourte A, Cherifi C, Maillet J, et al. Systemic inhibition of IL-6/STAT3 signalling protects against experimental osteoarthritis. *Ann Rheum Dis* 2017;76:748–55.
- van der Kraan PM, van den Berg WB. Osteophytes: relevance and biology. *Osteoarthritis Cartilage* 2007;15:237–44.
- David V, Laroche N, Boudignon B, et al. Noninvasive in vivo monitoring of bone architecture alterations in hindlimb-unloaded female rats using novel three-dimensional microcomputed tomography. *J Bone Miner Res* 2003;18:1622–31.
- Lepetsos P, Papavassiliou AG. ROS/oxidative stress signaling in osteoarthritis. *biochim biophys acta BBA. Mol Basis Dis* 2016;1862:576–91.
- Kim M-J, Kim H-J, Hong Y-H, et al. Age-Related NADPH oxidase (arnox) activity correlated with cartilage degradation and bony changes in age-related osteoarthritis. *J Korean Med Sci* 2015;30:1246–52.
- Hwang HS, Park IY, Hong JI, et al. Comparison of joint degeneration and pain in male and female mice in DMM model of osteoarthritis. *Osteoarthritis Cartilage* 2021;29:728–38.
- Wegner AM, Campos NR, Robbins MA, et al. Acute changes in NADPH oxidase 4 in early post-traumatic osteoarthritis. *J Orthop Res* 2019;37:2429–36.
- Kruisbergen NNL, Di Ceglie I, van Gemert Y, et al. Nox2 deficiency reduces cartilage damage and ectopic bone formation in an experimental model for osteoarthritis. *Antioxidants (Basel)* 2021;10:1660.
- Hu Y, Chen X, Wang S, et al. Subchondral bone microenvironment in osteoarthritis and pain. *Bone Res* 2021;9:20.

- 37 Bobinac D, Marinovic M, Bazdulj E, *et al.* Microstructural alterations of femoral head articular cartilage and subchondral bone in osteoarthritis and osteoporosis. *Osteoarthritis Cartilage* 2013;21:1724–30.
- 38 Buckland-Wright C. Subchondral bone changes in hand and knee osteoarthritis detected by radiography. *Osteoarthritis Cartilage* 2004;12 Suppl A:S10–9.
- 39 Lin C, Shao Y, Zeng C, *et al.* Blocking PI3K/Akt signaling inhibits bone sclerosis in subchondral bone and attenuates post-traumatic osteoarthritis. *J Cell Physiol* 2018;233:6135–47.
- 40 Tang P, Sheng J, Peng X, *et al.* Targeting nox4 disrupts the resistance of papillary thyroid carcinoma to chemotherapeutic drugs and lenvatinib. *Cell Death Discov* 2022;8:177.
- 41 Yu T, Li L, Liu W, *et al.* Silencing of NADPH oxidase 4 attenuates hypoxia resistance in neuroblastoma cells SH-SY5Y by inhibiting PI3K/Akt-dependent glycolysis. *Oncol Res* 2019;27:525–32.
- 42 Yu S-M, Kim S-J. The thymoquinone-induced production of reactive oxygen species promotes dedifferentiation through the ERK pathway and inflammation through the p38 and PI3K pathways in rabbit articular chondrocytes. *Int J Mol Med* 2015;35:325–32.
- 43 Hu Y, Gui Z, Zhou Y, *et al.* Quercetin alleviates rat osteoarthritis by inhibiting inflammation and apoptosis of chondrocytes, modulating synovial macrophages polarization to M2 macrophages. *Free Radic Biol Med* 2019;145:146–60.
- 44 Canton M, Sánchez-Rodríguez R, Spera I, *et al.* Reactive oxygen species in macrophages: sources and targets. *Front Immunol* 2021;12:734229.
- 45 Li D, Ni S, Miao K-S, *et al.* Pi3K/Akt and caspase pathways mediate oxidative stress-induced chondrocyte apoptosis. *Cell Stress Chaperones* 2019;24:195–202.
- 46 Song Y, Hao D, Jiang H, *et al.* Nrf2 regulates CHI3L1 to suppress inflammation and improve post-traumatic osteoarthritis. *J Inflamm Res* 2021;14:4079–88.
- 47 Marchev AS, Dimitrova PA, Burns AJ, *et al.* Oxidative stress and chronic inflammation in osteoarthritis: can Nrf2 counteract these partners in crime? *Ann N Y Acad Sci* 2017;1401:114–35.
- 48 Rashdan NA, Lloyd PG. Fluid shear stress upregulates placental growth factor in the vessel wall via NADPH oxidase 4. *Am J Physiol Heart Circ Physiol* 2015;309:H1655–66.
- 49 Sánchez-Gómez FJ, Calvo E, Bretón-Romero R, *et al.* Nox4-dependent hydrogen peroxide promotes shear stress-induced SHP2 sulfenylation and enos activation. *Free Radic Biol Med* 2015;89:419–30.
- 50 Goettsch C, Babelova A, Trummer O, *et al.* NADPH oxidase 4 limits bone mass by promoting osteoclastogenesis. *J Clin Invest* 2013;123:4731–8.